Magnetic and structural properties of epitaxial c-FeSi films grown on MgO(100)

M. Walterfang, W. Keune,* K. Trounov, and R. Peters
Fachbereich Physik, Universität Duisburg-Essen, D-47048 Duisburg, Germany

U. Rücker
Forschungszentrum Jülich, Institut für Festörperforschung, D-52425 Jülich, Germany

K. Westerholt
Institut für Experimentalphysik/Festkörperphysik, Universität Bochum, D-44780 Bochum, Germany
(Received 30 July 2005; revised manuscript received 3 March 2006; published 13 June 2006)

Conversion electron Mössbauer spectroscopy (CEMS) and superconducting quantum interference device (SQUID) magnetometry have been applied to study the metastable iron monosilicide phase (c-FeSi) with the B2 (or CsCl) lattice structure synthesized by molecular beam epitaxy (MBE). Thin films of nominal composition of c-$FeSi_{0.85}$ were grown by codeposition of ^{57}Fe and Si onto MgO(100) carrying a thin Fe or Cr buffer layer. X-ray diffraction was performed to determine the structure and epitaxial relationship of the c-$FeSi_{0.85}$(100) films. The B2 structure was observed after different thermal annealing steps. The lattice parameter perpendicular to the film plane was found to be 2.77(5) Å in each case. The CEM spectra at room temperature could be decomposed into two components: (i) a weakly quadrupole-split doublet assigned to nonmagnetic stoichiometric c-FeSi, and (ii) a weakly ferromagnetic component characterized by a distribution of hyperfine magnetic fields, $P(B_{hf})$, assigned to a fraction of nonstoichiometric c-$FeSi_x$ with excess Fe. CEMS and SQUID magnetometry demonstrate the occurrence of magnetic ordering effects with decreasing temperature down to 4.2 K. Our results reveal that, contrary to expectation, the stoichiometric c-FeSi phase is paramagnetic at room temperature and ferromagnetically ordered below ~30 K, while c-$FeSi_x$ is ferromagnetic at and below 300 K. At 5 K we find small ground-state Fe atomic magnetic moments μ_{Fe} of $(0.10\pm0.02)\ \mu_B$ for c-FeSi and $(0.13\pm0.03)\ \mu_B$ for c-$FeSi_x$. These small moments are reflected in the observed small hyperfine magnetic fields of 2~4 T in the ground state.

DOI: 10.1103/PhysRevB.73.214423 PACS number(s): 75.70.Ak, 75.50.Bb, 64.60.My, 76.80.+y

I. INTRODUCTION

During the last several years, iron silicides have attracted increasing interest from the fundamental as well as the technological points of view. One of the most relevant features of these materials is that, in addition to bulk phases,[1] metastable phases can be stabilized through epitaxial growth on a suitable substrate. The enhanced stability of metastable phases is mainly due to their better lattice matching with the substrate, giving it an advantage over the bulk stable phase because of the favorable interface contribution to the total energy.[2] These phases exhibit interesting properties not found in the bulk compounds. Moreover, metastable epitaxial phases have the basic interest of being crystallographically simpler than the bulk phases. They often represent ideal phases prior to instability driven deformations. The c-FeSi phase, which is considered to be nonmagnetic at room temperature (RT),[3–5] has the B2 (or CsCl) structure with space group $Pm\bar{3}m$, i.e., a simple-cubic lattice with a basis of Fe at the origin and Si at (1/2 1/2 1/2). Both atoms are coordinated with eight nearest neighbors.[6] The corresponding stable bulk phase, ϵ-FeSi, of this material is simple cubic and has $P2_13(T^4)$ space-group symmetry.[6]

Previously, the successful synthesis of metastable c-FeSi by molecular beam epitaxy (MBE) on both Si(111) (Ref. 7) and MgO(100) substrates[8] was reported. c-FeSi formation after ion implantation was observed by Reuther.[9,10] Furthermore, the c-FeSi phase has been observed in MBE-grown Fe/FeSi/Fe sandwiches.[11–13] Such structures are attracting interest due to strong antiferromagnetic coupling through the c-FeSi interlayer, which is of significance for applications in magnetoelectronics. Croonenborghs *et al.*[11] have studied the interlayer exchange coupling in MBE-grown Fe/c-$Fe_{0.50}Si_{0.50}$/Fe trilayers. Both the bilinear and the biquadratic coupling coefficient increase strongly with decreasing temperature down to ~70 K, but, surprisingly, then slightly decrease again. This behavior was explained within the framework of Slonczewski's loose spin model,[14] assuming a temperature-dependent concentration of paramagnetic entities.[11] Below ~100 K, the fractional loose spin concentration was found to decrease on cooling, but the reason for this behavior was left open.[11]

In this paper, we present a detailed study of the hitherto unknown low-temperature magnetic properties of metastable c-FeSi thin films grown on MgO(100) by MBE. ^{57}Fe conversion electron Mössbauer spectroscopy (CEMS) was performed between RT and 4.2 K in order to investigate structural and magnetic properties on an atomistic scale. Mössbauer spectroscopy is a powerful method for the study of local magnetic interactions as well as local structure and symmetry via magnetic and electric hyperfine (hf) interactions.[15] Because of the high sensitivity of the Mössbauer spectra with respect to the atomic and electronic surroundings of the ^{57}Fe probe nucleus, this method is very useful for the analysis of metallurgical phases. Complementary results from x-ray diffraction (XRD) and superconducting quantum interference device (SQUID) magnetometry studies are also presented. Our combined Mössbauer spectroscopical and SQUID results prove that, contrary

to expectation, the stoichiometric c-FeSi phase in the thin film develops ferromagnetism with a weak atomic moment and a small hyperfine magnetic field at low temperature. Our results suggest that the nonmonotonic temperature dependence of the bilinear and biquadratic coupling coefficients in Fe/c-FeSi/Fe trilayers, as observed in Ref. 11, is caused by the ferromagnetic behavior of the c-FeSi phase at low temperature.

II. EXPERIMENTAL

The c-FeSi phase was synthesized in a MBE system. The MgO(100)-substrate surface was first cleaned by using isopropanol and then [after insertion into the ultrahigh vacuum (UHV) system] by heating at 630 °C for 1 h to remove surface contaminants. The base pressure was 5×10^{-10} mbar. Two different samples were prepared. For sample 1, a 30 Å thick Fe buffer layer of natural isotopical composition was grown at 200 °C on MgO first, before growing a 135 Å thick $^{57}FeSi_{0.85}$ layer (nominally c-$^{57}Fe_{0.54}Si_{0.46}$ with 4 at. % excess Fe) at RT by co-deposition of ^{57}Fe and Si. The pressure during growth was 5×10^{-9} mbar. The deposition rates were 0.02 Å/s (^{57}Fe) and 0.029 Å/s (Si). For sample 2, a 30 Å thick Cr buffer layer was grown at 200 °C on MgO followed by a 150 Å thick $^{57}FeSi_{0.85}$ layer grown at RT by co-deposition of ^{57}Fe and Si. The deposition rates were 0.1 Å/s (^{57}Fe) and 0.145 Å/s (Si). Subsequently, sample 2 was annealed in UHV at 250 °C for 20 min. Finally, the samples were covered with a 50 Å thick Si layer (sample 1) and a 50 Å thick Cr layer (sample 2) for protection. High-purity materials (natural Fe: 99.9985 at. %, ^{57}Fe: 99.95 at. %, Cr: 99.999 at. %) were evaporated from resistively heated Knudsen cells, while Si (99.999 at. %) was evaporated from an electron gun. The deposition rates of ^{57}Fe (of 95% isotopical enrichment) and Si and the film thicknesses were measured by two independent calibrated quartz crystal oscillators. The composition given for the samples is the nominal composition as determined by the quartz crystal oscillators. As we have shown in prior work, the formation of a nearly undistorted stoichiometric c-FeSi phase after annealing is favored by excess Fe in the FeSi film, and is delayed by excess Si.[16] The samples were investigated *ex situ* after annealing for 20 min in UHV in different stages up to 250 °C (sample 1) and 310 °C (sample 2).

Mössbauer CEM spectra were measured at RT by mounting the sample in a He/CH_4-proportional counter, and by using a ^{57}Co source (Rh matrix). Low-temperature CEM spectra were obtained by using a channeltron electron detector placed, together with the sample, in the inner evacuated chamber of a liquid-He bath cryostat. The incident γ radiation was perpendicular to the sample surface. For the least-squares fitting of the CEM spectra, the NORMOS computer program by Brand[17] was used, which is based on the histogram method by Hesse and Rubartsch.[18] Θ-2Θ x-ray diffraction (XRD) was performed *ex situ* at RT and 113 K by using a Cu anode and a graphite monochromator ($\lambda_{K\alpha}$ = 1.54178 Å). Magnetic measurements were performed using a commercial SQUID (superconducting quantum interference device) magnetometer (Quantum Design MPMS).

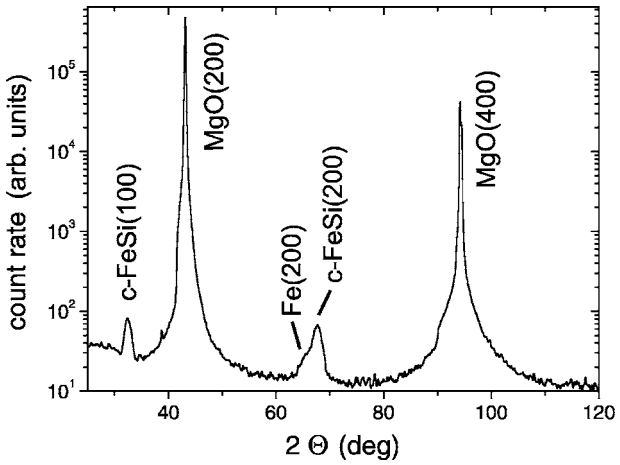

FIG. 1. Θ-2Θ x-ray diffraction diagram of the 250 °C annealed nominal c-$FeSi_{0.85}$ film (sample 1) at RT.

The epitaxial growth was checked by RHEED (reflection high-energy electron diffraction) on a sample that was similar to sample 2 and prepared under the same conditions as sample 2, but without a Cr cap layer. This sample was exposed to air during its transfer to the RHEED-UHV chamber, and RHEED was obtained after cleaning the sample surface by Ar ion sputtering at 0.5 keV at a sample temperature of 120 °C. After this treatment only Fe and Si (and no O) was detected by Auger electron spectroscopy.

III. RESULTS AND DISCUSSION

A. Structural investigations

XRD measurements were performed to determine the structure and epitaxial relationship of the nominal c-$FeSi_{0.85}$ films after annealing at 250 °C (sample 1) and 310 °C (sample 2), respectively. The XRD pattern of sample 1 is shown in Fig. 1. (The XRD pattern of sample 2 looks very similar and is not displayed.) We clearly observe Bragg-peaks at 32.35° and 67.69° corresponding to the c-FeSi(100) and c-FeSi(200) reflections, while at 65.10° the Fe(200) reflection is visible as a shoulder. The (n00) peaks are the only observable reflections due to the epitaxial relation c-FeSi(100)$\|$MgO(100) of the film. A proof of epitaxial growth is provided by the RHEED reflections taken along the c-FeSi[010] direction and shown in Fig. 2. RHEED reflections were observed also along other azimuthal directions (not shown). For the c-FeSi film of samples 1 and 2, a value of 2.77(5) Å (at RT) for the lattice spacing perpendicular to the surface was deduced byXRD. This agrees well with the value of 2.774 Å for c-FeSi films also grown on MgO(100), as found by Degroote *et al.*[8] Degroote *et al.*[8] have computed a theoretical value of 2.785 Å for the lattice spacing perpendicular to the surface of c-$FeSi_{0.85}$ with an undistorted cubic lattice cell. Our perpendicular lattice parameter obtained for the c-$FeSi_{0.85}$ film is slightly smaller (2.77 Å) than this calculated value. This may be explained by an increase of the atomic distances in the surface plane of the silicide layer induced by the lattice mismatch of −3.5% with the

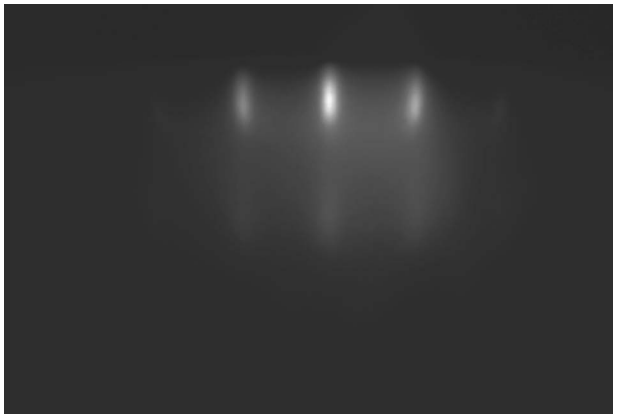

FIG. 2. RHEED pattern of an uncoated 150 Å thick nominal c-$FeSi_{0.85}$(100) film taken along the [010] azimuthal direction. (Electron energy: 10 keV.)

MgO(100) substrate, causing a decrease of the lattice spacing perpendicular to the surface.

Energy dispersive x-ray analysis (EDX) revealed that the 135 Å thick nominal c-$FeSi_{0.85}$ layer (sample 1) and the 150 Å thick nominal c-$FeSi_{0.85}$ layer (sample 2) both consist of lateral areas, which are a few microns large of stoichiometric c-FeSi and of nonstoichiometric c-$FeSi_x$ with excess Fe atoms. The Fe concentrations of the more Fe-rich areas of sample 2 were found to fluctuate betweeen 54 and 60 at. % ($\approx$ c-$FeSi_{0.75}$ in the average). In the case of sample 1, the total Fe and Si content (Fe buffer layer+c-$FeSi_{0.85}$ +Si-cap layer) was measured. Therefore, the calculated Fe concentration of 52 at. % of the more Fe-rich areas inside the iron-silicide layer of sample 1 (corresponding to c-$FeSi_{0.93}$) may contain a systematic error, as assumptions had to be made. An independent estimation of the sample composition was made via the known isomer-shift–vs–Si-concentration relationship (see Sec. III B). This yields an Fe concentration of c-$FeSi_x$ in sample 1 of (54±5) at. % Fe.

This lateral inhomogeneity in the sample composition is reflected also in the Mössbauer spectra by the appearance of two different subspectra (see Sec. III B). (Throughout the paper we will give the nominal sample composition.) A deviation from the nominal Fe/Si concentration ratio was also obtained by Degroote *et al.*[8] By stoichiometric codeposition of Fe and Si at RT, these authors grew thin c-FeSi films with different thicknesses between 90 and 580 Å on a 30 Å thick Fe buffer layer on MgO(100). From Rutherford backscattering spectrometry (RBS), they observed a Fe excess of ~4 at. % (c-$^{57}Fe_{0.54}Si_{0.46}$ or $FeSi_{0.85}$) for all silicide layers of the different samples.

B. Mössbauer spectroscopy

The CEM spectra of the 135 Å thick nominal c-$FeSi_{0.85}$ film (sample 1) in the as-grown state and after annealing at different temperatures are shown in Figs. 3(a)–3(c). The obtained fitting parameters are reported in Table I. All spectra were least-squares fitted with two spectral components: (i) one asymmetric quadrupole-split doublet (labeled D1) with Lorentzian line shape [following the work by Croonenborghs

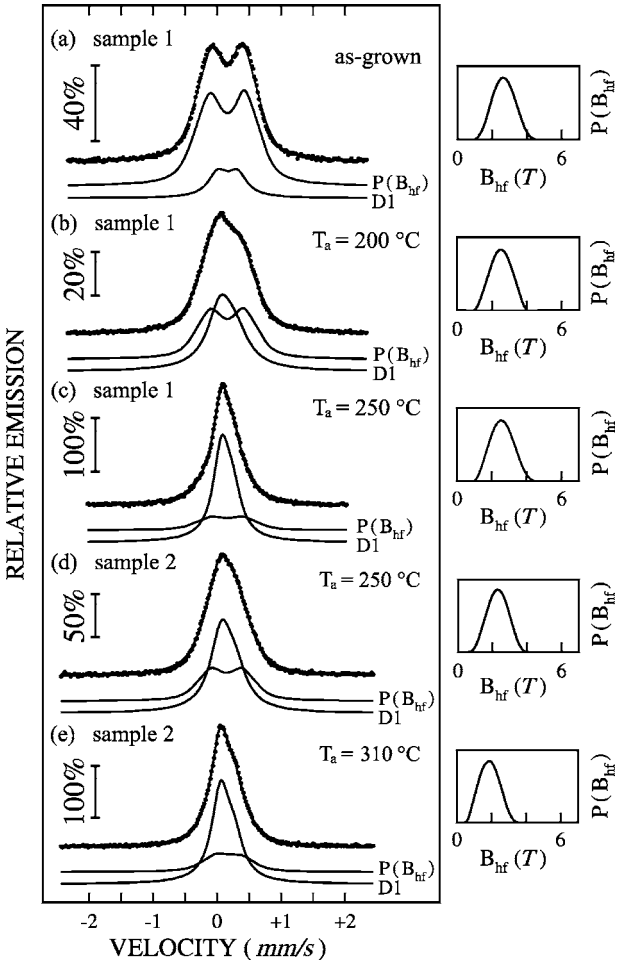

FIG. 3. CEM spectra of the nominal c-$FeSi_{0.85}$ film (sample 1) measured at RT in the as-grown state (a) and after annealing at 200 °C (b) and 250 °C (c). CEM spectra of the nominal c-$FeSi_{0.85}$ film (sample 2) measured at RT after annealing at 250 °C (d) and 310 °C (e) are also shown. The spectra were fitted with a quadrupole doublet D1 and a magnetic hf field distribution, $P(B_{hf})$, right-hand side.

et al.,[20] we assumed an intensity ratio $I_</I_>>1$ for the intensity of the low ($I_<$) and high ($I_>$) energy line of the quadrupole doublet D1]; and (ii) a spectral component with a magnetic hf field distribution, $P(B_{hf})$. (A linear correlation between the hf field, B_{hf}, and the isomer shift, δ, had to be assumed to obtain a good fit.) With increasing annealing temperature, the spectral area of doublet D1 increases at the expense of that of the magnetic hf field distribution $P(B_{hf})$ (Figs. 3(a)–3(c) and Table I). After the 250 °C annealing, the relative spectral area (relative integrated intensity) of doublet D1 was found to be 79%, as compared to 18% in the as-grown state.

Figures 3(d) and 3(e) exhibit the CEM spectra of the 150 Å thick nominal c-$FeSi_{0.85}$ film (sample 2) after annealing at 250 and 310 °C, respectively. The spectra were again fitted with a doublet D1 and a component with a magnetic hf field distribution $P(B_{hf})$. Upon annealing from 250 °C up to 310 °C, the relative spectral area of doublet D1 increases at the expense of that of the magnetic hf field distribution

TABLE I. Mössbauer spectral parameters of samples 1 and 2 of nominal composition c-$FeSi_{0.85}$: isomer shift δ and mean isomer shift $\langle\delta\rangle$ relative to α-Fe at RT, linewidth Γ, quadrupole splitting ΔE_Q, ratio of the intensity of the high ($I_>$) and low ($I_<$) energy line of the quadrupole doublet, average magnetic hf field $\langle B_{\mathrm{hf}}\rangle$, and relative spectral area A. T is the measurement temperature and T_a the annealing temperature.

T (C)	T_a (K)	Subspectrum	δ (mm/s)	Γ (mm/s)	ΔE_Q (mm/s)	$I_</I_>$	$\langle\delta\rangle$ (mm/s)	$\langle B_{\mathrm{hf}}\rangle$ (T)	A (%)
Sample 1									
RT	As-grown	D1	0.26(3)	0.35(5)	−0.30	1.0			18
		$P(B_{\mathrm{hf}})$		0.30			0.26(8)	2.7(1)	82
RT	200	D1	0.28(4)	0.48(9)	−0.24(6)	2.4(1)			53
		$P(B_{\mathrm{hf}})$		0.30			0.27(7)	2.5(1)	47
RT	250	D1	0.26(6)	0.30(2)	−0.18(3)	2.3(2)			79
		$P(B_{\mathrm{hf}})$		0.30			0.25(2)	2.6(3)	21
RT	250	D1	0.27(3)	0.38(9)	−0.23(1)	2.3(1)			73
(B=0.95 T)		$P(B_{\mathrm{hf}})$		0.30			0.26(3)	1.8(3)	27
110	250	D1	0.37(1)	0.34(4)	−0.17(5)	2.3(3)			68
		$P(B_{\mathrm{hf}})$		0.30			0.30(5)	2.8(4)	32
4.2	250	D1	0.45(2)	0.33(8)	−0.26(3)	2.3(1)			16
		$P(B_{\mathrm{hf}})$		0.30			0.33(2)	5.6(5)	84
Sample 2									
RT	250	D1	0.28(3)	0.41(8)	−0.22(6)	2.4(3)			65
		$P(B_{\mathrm{hf}})$		0.30			0.25(3)	2.3(2)	35
RT	310	D1	0.26(5)	0.33(3)	−0.21(1)	2.4(1)			77
		$P(B_{\mathrm{hf}})$		0.30			0.24(3)	1.9(3)	23
80	310	D1	0.38(7)	0.33(2)	−0.21(3)	2.4(2)			63
		$P(B_{\mathrm{hf}})$		0.30			0.36(1)	2.4(2)	37
4.2	310	D1	0.40(7)	0.33(3)	−0.21(1)	2.4(1)			17
		$P(B_{\mathrm{hf}})$		0.30			0.36(4)	3.8(1)	83

$P(B_{\mathrm{hf}})$ from 65% to 77% [Figs. 3(d) and 3(e) and Table I].

The hf parameters of doublet D1 cannot be assigned to any known stable Fe-Si phase.[19] Upon annealing up to 250 °C (sample 1) and 310 °C (sample 2) the isomer shift of doublet D1 remains nearly unchanged (Table I). The value of the isomer shift (0.26 mm/s for both samples) after annealing corresponds to values reported in the literature for the metastable c-FeSi phase, which ranges from 0.24 to 0.26 mm/s.[6,8] The point symmetry at the Fe site in the B2 structure is O_h, and therefore, no quadrupole interaction is expected and a single line should be observed. However, in the as-grown state as well as in the annealed state no single line is observed, but instead the doublet D1 with a small quadrupole splitting $|\Delta E_Q|$ (of ~0.18 and ~0.21 mm/s at RT in the annealed state of samples 1 and 2, respectively) appears. The origin of a quadrupole doublet is the hf splitting of the first excited ^{57}Fe nuclear energy level induced by an electric field gradient (EFG) at the site of the ^{57}Fe nucleus. An EFG can only occur at a site with lower than cubic symmetry. Therefore, the quadrupole splitting of the D1 doublet is related to a small local tetragonal distortion induced by lattice strain due to the lattice mismatch of −3.5% with the MgO(100) substrate, as recently observed by Croonenborghs *et al.*[20] They found that in the case of (001) oriented growth the principal axis of the EFG (V_{zz}) is parallel to the [001] direction with a negative sign of the principal value V_{zz} of the EFG, corresponding to a negative sign of $\Delta E_Q = \frac{1}{2}eQV_{zz}$ (Q=quadrupole moment of the ^{57}Fe nucleus in the excited state). The negative sign of the quadrupole splitting ΔE_Q in c-FeSi (Table I) has been inferred by measuring the angular dependence of the intensity ratio, I_π/I_σ, of the two transitions I_π ($m=\pm 1/2 \rightarrow \pm 3/2$) and I_σ ($m=\pm 1/2 \rightarrow \pm 1/2$) of the quadrupole doublet for our sample 1 (not shown). For the intensity ratio of the low-energy ($I_\pi=I_<$) to the high-energy ($I_\sigma=I_>$) Mössbauer line, we obtained values of 2.33 (for $\theta=0$) and 0.92 (for $\theta=60$), where θ is the angle between the film normal direction and the incident γ-ray direction. These values are consistent with $V_{zz}<0$ and a preferred direction of V_{zz} perpendicular to the film plane.[20] Our result confirms the earlier findings of Ref. 20.

Moreover, a general tendency for strain relaxation with increasing layer thickness was observed.[20] Because of our thicker c-FeSi films, the RT values of the quadrupole splitting [ΔE_Q=−0.18 mm/s (sample 1 after annealing at 250 °C) and ΔE_Q=−0.21 mm/s (sample 2 after annealing at 310 °C)] are slightly smaller in magnitude than the corresponding value of −0.26 mm/s obtained by Croonenborghs *et al.*[20] for a Fe(80 Å)/c-^{57}FeSi(30 Å)/Fe(40 Å) sandwich grown on MgO(100) by MBE. The proportional constant be-

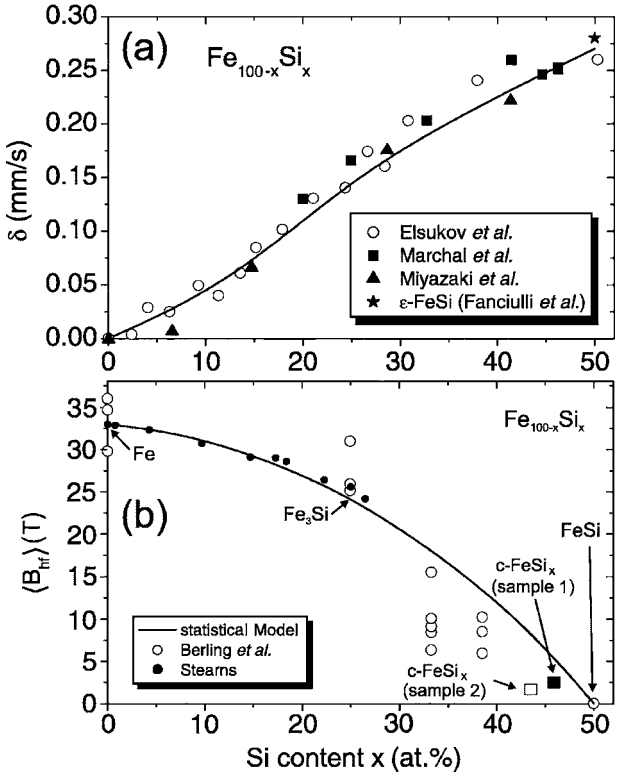

FIG. 4. (a) Correlation between isomer shift δ and Si concentration, determined from CEMS measurements on $Fe_{100-x}Si_x$ layers. The full drawn curve is a guide for the eyes. (b) Si-concentration dependence of the average magnetic hf field, $\langle B_{hf}\rangle$, at the ^{57}Fe nucleus for $Fe_{100-x}Si_x$ at RT. The full-drawn curve corresponds to the statistical model (Ref. 3).

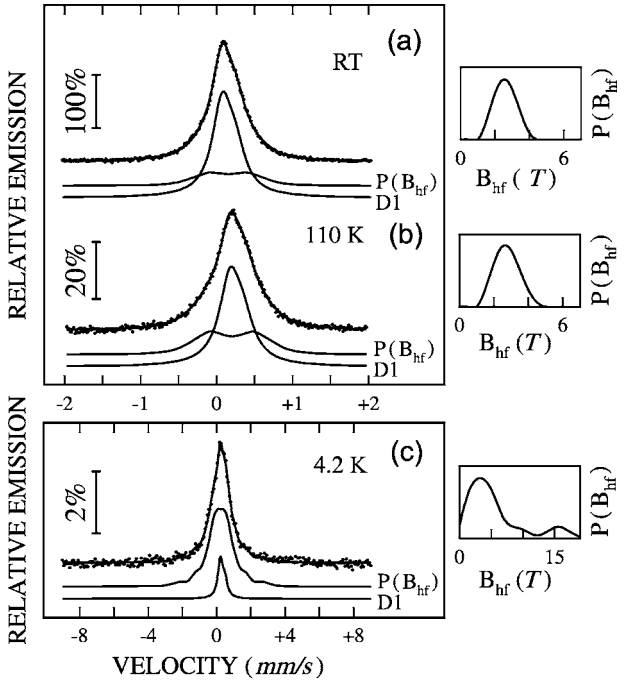

FIG. 5. CEM spectra of the 250 °C annealed nominal c-$FeSi_{0.85}$ film (sample 1) measured at RT, 110 and 4.2 K. The spectra were fitted with an asymmetrical doublet D1 and a component with a magnetic hf field distribution, $P(B_{hf})$, right-hand side. Note the different velocity scales in (a) and (b) as compared to (c). The apparent width of the measured feature increases upon cooling.

tween the tetragonal distortion $\epsilon_T = \epsilon^{\parallel} - \epsilon^{\perp}$ and ΔE_Q was given in Ref. 20 as $-18.5(9)\ \%/\mathrm{mms}^{-1}$. Using this value, we obtain a tetragonal distortion ϵ_T of 3.3% and 3.9% in the c-$FeSi_{0.85}$ film of our samples 1 and 2, respectively.

CEMS measurements at RT on $Fe_{100-x}Si_x$ layers performed by Elsukov *et al.* (crystalline layers),[21] Marchal *et al.*[22] and Mangin and Marchal[23] (amorphous layers), Miyazaki *et al.*[24] ($0 \le x \le 22.7$: crystalline, $28.4 \le x \le 41$: amorphous) revealed a correlation between isomer shift and Si concentration, which is summarized in Fig. 4(a); additionally, a data point for the isomer shift of ϵ-FeSi obtained by Fanciulli *et al.*[6] is plotted. It follows from this correlation that an isomer shift of 0.26(6) mm/s (as for doublet D1 of samples 1 and 2, Table I) corresponds to a Fe content of ~50 at. %. Thus, doublet D1 represents the stoichiometric c-FeSi phase. Correspondingly, the Fe content of the nonstoichiometric c-$FeSi_x$ phase [represented by the magnetic hf field distribution $P(B_{hf})$ with $\langle\delta\rangle = 0.25(2)$ mm/s (sample 1) and $\langle\delta\rangle = 0.24(3)$ mm/s (sample 2)] was found to be ~ (54±5) at % (≈c-$FeSi_{0.85}$, sample 1) and ~ (57±5) at % (≈c-$FeSi_{0.75}$, sample 2), being in agreement with the EDX results within error bars.

The origin of the magnetic hf field distribution, $P(B_{hf})$, representing the nonstoichiometric c-$FeSi_x$ phase is attributed to the fact that thin $Fe_{100-x}Si_x$ films are ferromagnetic at RT for $0 \le x < 50$. Figure 4(b) exhibits the correlation between the average magnetic hf field, $\langle B_{hf}\rangle$, at the ^{57}Fe nucleus and the Si concentration for thin $Fe_{100-x}Si_x$ layers at RT. The solid line results from a calculated statistical model for bcc Fe-Si alloys as described in Ref. 3. Also shown are values determined by various experimental techniques [Berling *et al.*:[3] MOKE (magneto-optic Kerr effect) and XMCD (x-ray magnetic circular dichroism), as well as Stearns[25] and Elsukov *et al.*:[21] transmission Mössbauer spectroscopy). The local magnetic moments μ_{Fe} of the Fe atoms measured by Berling *et al.*[3] were converted into B_{hf} values by using the well-known conversion factor of 15 T/μ_B for bcc-Fe alloys.[26] The hf field distribution reveals an average magnetic hf field, $\langle B_{hf}\rangle$, of 2.6 T for c-$FeSi_{0.85}$ (sample 1) and 1.9 T for c-$FeSi_{0.75}$ (sample 2), both at RT (Table I), which agrees with the statistical model [Fig. 4(b)]. Therefore, it can be concluded that the Fe atoms of the nonstoichiometric c-$FeSi_x$ phase have a small magnetic moment and are magnetically ordered at RT.

The CEM spectra of the nominal c-$FeSi_{0.85}$ film (sample 1) after 250 °C annealing, measured at RT, 110 and 4.2 K, are shown in Fig. 5. Again, the spectra were fitted with an asymmetric quadrupole doublet (D1) and a magnetic hf field distribution, $P(B_{hf})$. With decreasing temperature, the relative spectral area A of doublet D1 decreases from 79% at RT to 16% at 4.2 K, while the spectral area of the magnetic hf field distribution $P(B_{hf})$ increases correspondingly from 21% at RT to 84% at 4.2 K (Table I and Fig. 5). A similar effect upon cooling is observed for the nominal c-$FeSi_{0.85}$ film (sample 2) after 310 °C annealing. The corresponding spec-

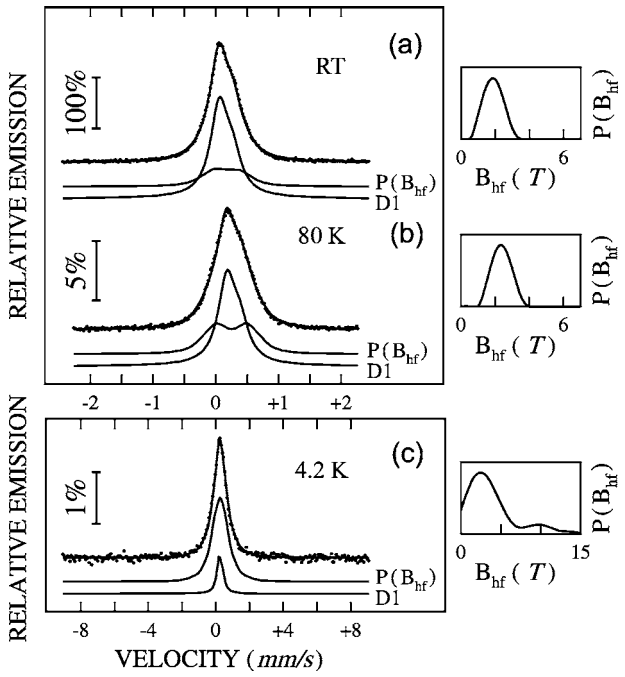

FIG. 6. CEM spectra of the 310 °C annealed nominal c-$FeSi_{0.85}$ film (sample 2) measured at RT, 80 and 4.2 K. The spectra were fitted with an asymmetrical doublet D1 and a component with a magnetic hf field distribution, $P(B_{hf})$, right-hand side. The apparent width of the measured feature increases upon cooling.

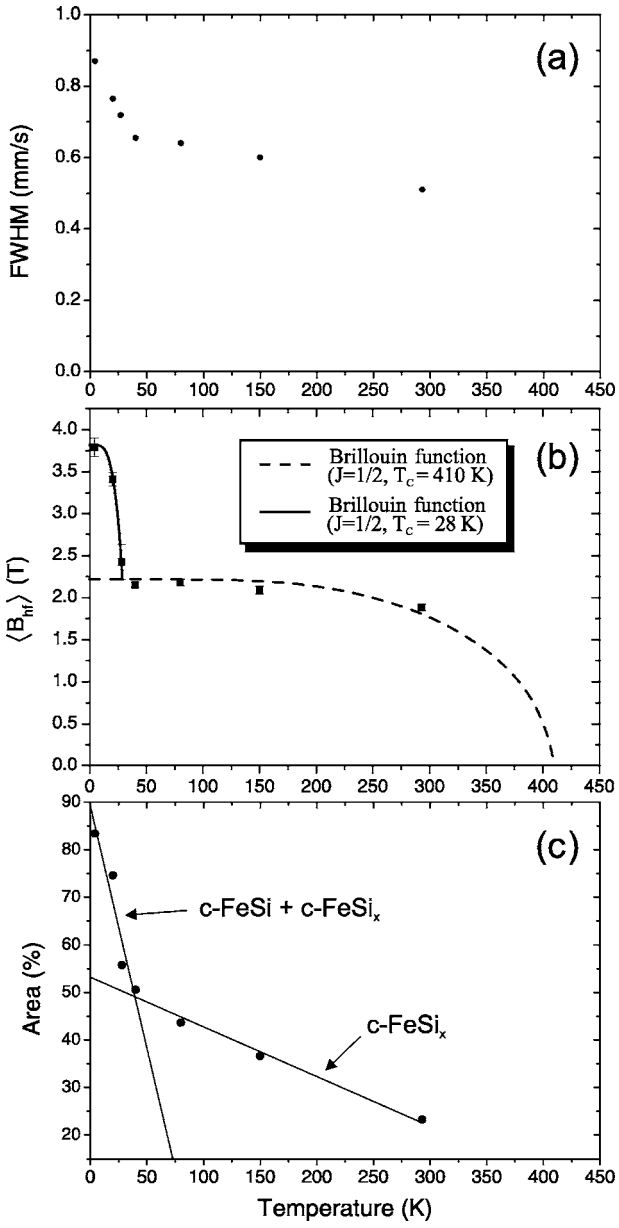

FIG. 7. Apparent full width at half maximum (FWHM) of the CEM spectrum (a), average magnetic hf field $\langle B_{hf}\rangle$ (b), and relative spectral area of the magnetic spectral component $P(B_{hf})$ (c) of the 310 °C annealed nominal c-$FeSi_{0.85}$ film (sample 2) as a function of the measurement temperature. The dashed curve (full-drawn curve) in (b) is a least-squares fit with a Brillouin function $\left(J=\frac{1}{2}\right)$ of the data points above 28 K (below 28 K). The fits result in $T_C \approx 410$ K (for nonstoichiometric c-$FeSi_x$) and $T_C \approx 28$ K (for stoichiometric c-FeSi) in sample 2. The straight lines in (c) are least-squares fits to the data points.

tra measured at RT, 80 and 4.2 K are presented in Fig. 6. The spectral area of doublet D1 decreases from 77% at RT to 17% at 4.2 K, while the area of the magnetic hf field distribution $P(B_{hf})$ increases correspondingly from 23% at RT to 83% at 4.2 K. Simultaneously, the apparent line width of the measured spectra [full width at half maximum (FWHM)] is observed to increase on cooling [Fig. 7(a)].

Concerning our Mössbauer analysis, the crucial question is whether our assumption of a magnetic hf field distribution $P(B_{hf})$ for one of the spectral components is justified, and whether the overall apparent broadening of the CEM spectra upon cooling [as observed in Figs. 5, 6, and 7(a)] is of magnetic origin (as we claim). Our Mössbauer analysis thus far implies that the decrease of the relative spectral area (or integrated relative intensity) of doublet D1 (Table I) and the corresponding increase of the relative spectral area of the component with hf field distribution, $P(B_{hf})$, upon cooling is related to a transformation of c-FeSi from a nonmagnetic state (doublet D1) to a magnetic state [related to $P(B_{hf})$] upon lowering the temperature. Increasing electrical quadrupole interactions might also contribute to the observed apparent line broadening upon cooling. This could be caused, for instance, by increasing inhomogeneous lattice distortions with decreasing temperature. Therefore, low-temperature XRD measurements in Θ-2Θ geometry at 113 K were performed to determine possible changes of the lattice parameter. The apparent line broadening was already remarkable at 113 K as compared to the width at RT (Figs. 5–7). The XRD patterns measured at RT and 113 K of the 250 °C annealed nominal c-$FeSi_{0.85}$ film (sample 1) are shown in Fig. 8. At RT, the c-FeSi(100) Bragg peak is located at $2\Theta = 32.33°$, while at 113 K the same peak is located at $2\Theta = 32.28°$. This small shift is due to thermal expansion effects. Moreover, both Bragg peaks exhibit the same linewidth. Thus, we conclude that anomalous inhomogeneous lattice distortions upon cooling are absent, and, consequently, that negligible anomalous quadrupole-interaction effects due to inhomogeneous lattice distortions occur in our samples upon decreasing the temperature.

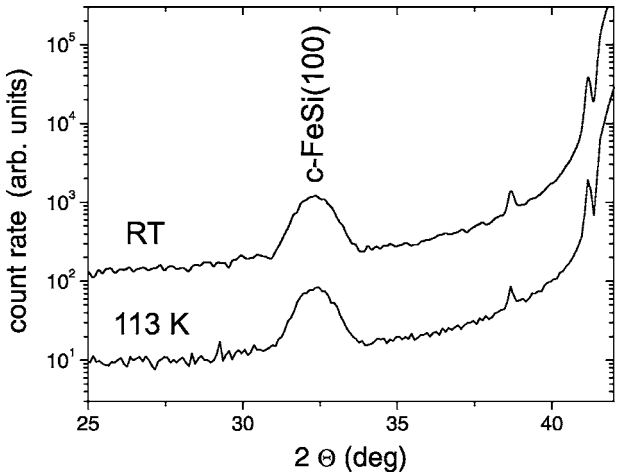

FIG. 8. Θ-2Θ x-ray diffraction diagram of the 250 °C annealed nominal c-$FeSi_{0.85}$ film (sample 1) measured at RT (upper diagram) and 113 K (lower diagram). For a better representation, the upper diagram is shifted to higher count-rate values.

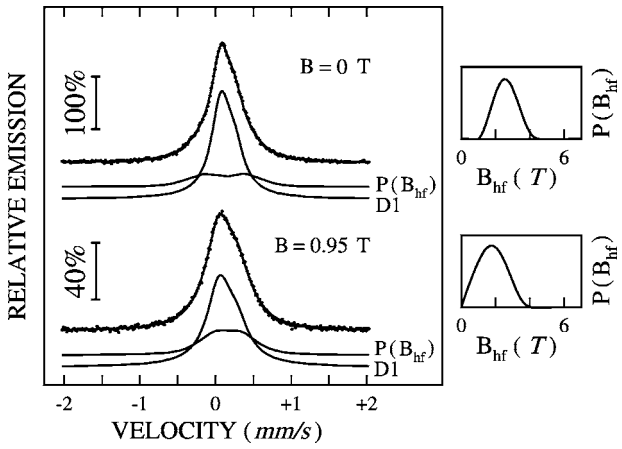

FIG. 9. CEM spectra of the 250 °C annealed nominal c-$FeSi_{0.85}$ film (sample 1) measured at RT without (B_{ext}=0 T) and within an external magnetic field B_{ext}=0.95 T applied in the film plane. The spectra were fitted with an asymmetric doublet D1 and a magnetic hf field distribution, $P(B_{hf})$, right-hand side.

A noticeable increase of the quadrupole splitting with decreasing temperature could also be caused by electronic band-structure effects, as previously observed for ϵ-FeSi,[27] for which a maximum quadrupole splitting of ΔE_Q =0.75 mm/s was measured at 4.2 K. A tentative fit (not shown) of the 4.2 K spectrum of sample 1 (250 °C annealed) with a quadrupole distribution $P(\Delta E_Q)$ resulted in a large average quadrupole splitting of $\langle \Delta E_Q \rangle$=0.97 mm/s, and a tail of the distribution extending up to ΔE_Q values of ~4 mm/s. However, such values are unphysically large for metallic systems, such as c-FeSi.

Thus, we are led to the conclusion that the observed line broadening during cooling cannot be attributed to electronic band-structure effects or to structural changes causing increased electric quadrupole interaction, but have to be related to magnetic ordering effects. In order to obtain further information on the latter aspect, additional CEMS measurements were performed at RT in an external magnetic field B_{ext} of 0.95 T applied in the film plane. The obtained CEM spectrum of sample 1 (250 °C annealed) is shown in Fig. 9. This spectrum was also fitted with an asymmetric doublet (D1) and a magnetic hf field distribution $P(B_{hf})$. The external magnetic field of 0.95 T causes only a small line broadening of doublet D1, while the average magnetic hf field $\langle B_{hf} \rangle$ of the nonstoichiometric c-$FeSi_x$ phase decreases by a value being nearly equal to the external applied field (Table I). Obviously, the nonstoichiometric c-$FeSi_x$ phase is ferromagnetic at RT and its Fe moments align nearly parallel to the B_{ext} direction, while the stoichiometric c-FeSi phase is dia- or paramagnetic at RT.

Figure 7(b) shows the temperature dependence of the average magnetic hf field, $\langle B_{hf} \rangle$, determined from the distribution $P(B_{hf})$. Between RT and ~30 K $\langle B_{hf} \rangle$ rises only slightly upon cooling, while below ~30 K down to 4.2 K a remarkable anomalous increase is observed. A similar behavior appears in the T dependence of the apparent spectral linewidth [Fig. 7(a)]. The unusual $\langle B_{hf} \rangle$ (T) behavior in Fig. 7(b) is explained by the presence of the two phases, the nonstoichiometric c-$FeSi_x$ phase and the stoichiometric c-FeSi phase, in sample 2 (and similarly in sample 1). According to Table I, the c-$FeSi_x$ phase is ferromagnetic at RT with a hf field of $\langle B_{hf} \rangle$=2.6 T (sample 1) or 1.9 T (sample 2), while the c-FeSi phase (doublet D1) is diamagnetic or paramagnetic at RT (diamagnetism can be excluded because of reasons given below). $\langle B_{hf} \rangle$ of the c-$FeSi_x$ phase increases slightly between RT and ~30 K because of increasing magnetic order by lowering T. The drastic increase of $\langle B_{hf} \rangle$ below ~30 K is due to the onset and increase of magnetic order of the stoichiometric c-FeSi phase upon cooling. It should be mentioned that this is the T range, where the relative spectral area of doublet D1 decreases strongly on behalf of the spectral area of the component described by $P(B_{hf})$. This is demonstrated in Fig. 7(c) for the case of sample 2. At 4.2 K, the CEM spectra are described essentially by only one hf distribution $P(B_{hf})$ because of the smallness of the magnetic hf fields and the limited spectral resolution. In other words, at low temperatures, $T \leq 30$ K, the hf distribution $P(B_{hf})$ averages over the magnetically ordered states of both phases, c-$FeSi_x$ and c-FeSi. It is obvious from the 4.2 K CEM spectra in Figs. 5 and 6 [and from Fig. 7(c) and Table I] that a small fraction of Fe atoms in the c-FeSi phase remains nonmagnetic even at 4.2 K, since a weak D1 doublet still persists, according to Figs. 5 and 6. This might be caused by small concentration inhomogeneities or defects in the films.

A similar effect upon cooling was also observed by Dekoster *et al.*[12] They prepared a 620 Å thick c-FeSi film on Si(111) by stoichiometric coevaporating of Fe and Si at RT. Because of the larger film thickness the Mössbauer spectrum in Ref. 12 exhibits a single line and not a quadrupole doublet. Cooling to 85 K did not alter the spectral shape. However, by further reducing the temperature down to 4.2 K in addition to the single line component, a broad spectral component was observed. Dekoster *et al.*[12] attributed this observation to the onset of magnetic ordering in the c-FeSi layer. Analysis of the magnetic spectral component in Ref. 12 resulted in an average magnetic hf field of $\langle B_{hf} \rangle$

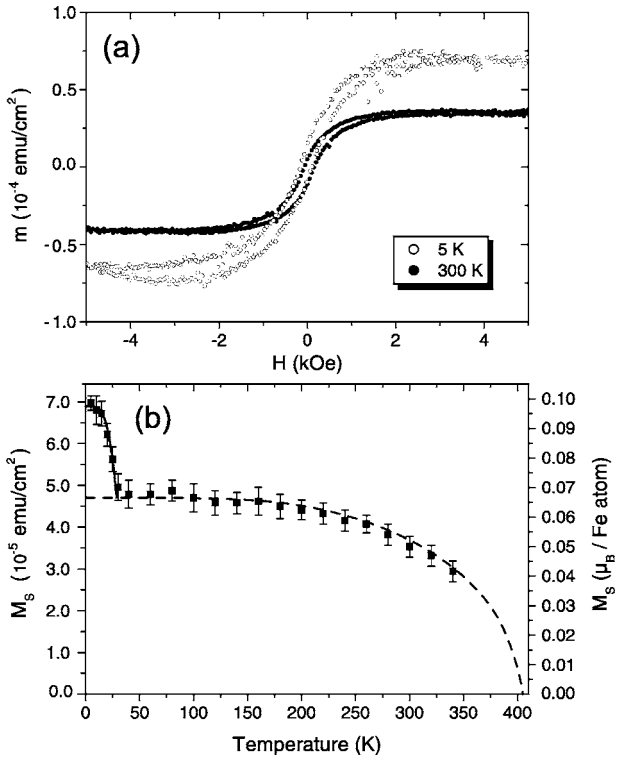

FIG. 10. In-plane magnetization curves (after subtraction of the diamagnetic background from the substrate), measured at RT and 5 K (a), and saturation magnetization M_S as a function of the measurement temperature (b), of the 310 °C annealed nominal c-$FeSi_{0.85}$ film (sample 2). The dashed curve (full-drawn curve) in (b) is a least-squares fit with a Brillouin function $(J=\frac{1}{2})$ of the data points above 28 K (below 28 K). The fits result in $T_C \approx 405$ K (for nonstoichiometric c-$FeSi_x$) and $T_C \approx 28$ K (for stoichiometric c-FeSi) in sample 2.

$=4.9(1)$ T. This is in fair agreement with our corresponding values[$\langle B_{\mathrm{hf}}\rangle = 5.6(5)$ T for sample 1 and $\langle B_{\mathrm{hf}}\rangle = 3.8(1)$ T for sample 2].

The data points plotted in Fig. 7(b) in the temperature range between RT and 28 K were fitted with a Brillouin function with $J=\frac{1}{2}$, resulting in a Curie temperature $T_C \approx 410$ K for the nonstoichiometric c-$FeSi_x$ phase. For this phase, an average saturation hf field of 2.2 T can be estimated by extrapolating to $T=0$ K in Fig. 7(b). In the T range below 28 K, the data points were fitted with the sum of two Brillouin functions with $J=\frac{1}{2}$ (with fitted parameters $T_C=410$ K for the nonstoichiometric c-$FeSi_x$ phase, and $T_C=28$ K for the stoichiometric c-FeSi phase). Thus, the magnetic ordering temperature T_C of the stoichiometric c-FeSi phase is ~28 K. The observation of magnetic ordering at low temperature constitutes indirect evidence that the stoichiometric c-FeSi in this thin film architecture is in a paramagnetic, rather than diamagnetic state.

C. Magnetometry

Complementary magnetic measurements were performed in order to prove magnetic ordering of the stoichiometric c-FeSi phase. Figure 10(a) shows typical magnetization curves of sample 2 (310 °C annealed) measured at RT and 5 K with the external field applied in the sample plane. The hysteresis loops observed in Fig. 10 prove that sample 2 is ferromagnetic at RT and at 5 K. The coercivity was found to be ~105 mT at RT and ~135 mT at 5 K. The temperature dependence of the saturation magnetization M_S shown in Fig. 10(b) is remarkably similar to the T dependence of the average magnetic hf field, $\langle B_{\mathrm{hf}}\rangle$ [Fig. 7(b)]. The data points plotted in Fig. 10(a) in the temperature range between RT and 28 K were fitted with a Brillouin function with $J=\frac{1}{2}$, resulting in a Curie temperature $T_C=405$ K for the nonstoichiometric c-$FeSi_x$ phase. This value is in very good agreement with $T_C=410$ K obtained from Fig. 7(b). In the temperature range below 28 K, the data points were fitted with the sum of two Brillouin functions with $J=\frac{1}{2}$, yielding $T_C=405$ K for the nonstoichiometric c-$FeSi_x$, and $T_C=28$ K for the stoichiometric c-FeSi. Thus, our results prove that stoichiometric c-FeSi is paramagnetic at RT and becomes ferromagnetically ordered below ~28 K.

As the film surface area, the film thickness and the nominal Fe concentration [(54±3) at. %] are known for sample 2, it is straightforward to calculate the average Fe atomic moment, $\langle \mu_{\mathrm{Fe}}\rangle$ (averaged over all Fe atoms, magnetic and nonmagnetic, in sample 2), from the $M_S(T)$ data in Fig. 10(b). The result is given on the right-hand-side vertical scale in Fig. 10(b). The $\langle \mu_{\mathrm{Fe}}\rangle$ values are relatively small: for instance, 0.067 μ_B at 40 K and at 0 K (extrapolated) for the c-$FeSi_x$ phase, and 0.098 μ_B at 5 K (for c-FeSi+c-$FeSi_x$). Mössbauer spectroscopy shows via the spectral area of the $P(B_{\mathrm{hf}})$ contribution that only 50.5% of all Fe atoms in the sample are magnetically ordered at 40 K [Fig. 7(c)], the rest being paramagnetic. This allows one to calculate the Fe atomic moment in the magnetically ordered c-$FeSi_x$ phase, μ_{Fe}(c-$FeSi_x$), to be (0.13±0.03) μ_B at 40 K and at $T=0$ K (extrapolated). A similar calculation for $T=5$ K, where according to the Mössbauer spectral area of Table I and Fig. 7(c) 83.3% of all Fe atoms in sample 2 are magnetically ordered (with the rest being paramagnetic), provides a value of (0.12±0.03) μ_B for the Fe atomic moment, μ_{Fe}(c-FeSi +c-$FeSi_x$) at 5 K, averaged over the magnetically ordered fractions of both phases, c-FeSi and c-$FeSi_x$.

In order to determine the Fe atomic moment of stoichiometric c-FeSi at 5 K, one has to know the fractions of magnetically ordered Fe atoms in c-FeSi and in c-$FeSi_x$, both at 5 K, separately. This is achieved via Fig. 7(c), where the observed linear T dependence of the Mössbauer spectral area A of magnetically ordered c-$FeSi_x$ is extrapolated to $T=5$ K. This gives a value $A=52.6\%$ for c-$FeSi_x$ at 5 K, i.e., 52.6% of all Fe atoms belong to magnetically ordered c-$FeSi_x$ at 5 K. Hence, according to Fig. 7(c), 83.3% −52.6% =30.7% of all Fe atoms belong to magnetic stoichiometric c-FeSi at 5 K. [The remainder (16.7% of all Fe atoms) is paramagnetic at 5 K]. Using these fractions of magnetically ordered Fe atoms, we obtain a value μ_{Fe}(c-FeSi)=(0.10±0.02) μ_B for stoichiometric c-FeSi and μ_{Fe}(c-$FeSi_x$)=(0.13±0.03) μ_B for nonstoichiometric c-$FeSi_x$, both at 5 K. These values can be regarded as the ground-state Fe magnetic moments ($T=0$ K); obviously, these values are relatively small and of the order of 0.1 μ_B.

This result, obtained from magnetometry, is qualitatively supported by the relatively small value of the observed hyperfine magnetic field, B_{hf}, of 3.8 T in sample 2 at 4.2 K [Table I and Fig. 7(b)]. By using the known conversion factor of ~ 15 T/μ_B for Fe alloys,[26] the hyperfine field provides a rough estimate of the Fe atomic moment of ~ 0.25 μ_B at 4.2 K (or in the ground state) for c-FeSi+c-FeSi$_x$. This value is of the same order of magnitude as μ_{Fe} determined from magnetometry.

As mentioned above, Croonenborghs *et al.*[11] found in MBE-grown Fe/c-$Fe_{0.50}Si_{0.50}$/Fe trilayers a strong increase of the bilinear coupling coefficient with decreasing temperature from RT down to ~ 70 K, and a slight decrease on further cooling. Because of the ferromagnetic ordering of the stoichiometric c-FeSi phase upon cooling, one would expect at low temperature no antiferromagnetic interlayer coupling in Fe/FeSi multilayers at all. Gareev *et al.*,[28] who have studied the interlayer exchange coupling in MBE-grown Fe/$Fe_{1-x}Si_x$/Fe trilayers, found that $Fe_{0.56}Si_{0.44}$ spacers also show antiferromagnetic interlayer coupling at low temperature. Similar to the observations of Croonenborghs *et al.*,[11] the bilinear coupling coefficient strongly increases with decreasing temperature and levels off below 80 K in Ref. 29. From literature[3,5] and our SQUID measurement of sample 2 [Fig. 10(a)], it is known that $Fe_{0.56}Si_{0.44}$ films are ferromagnetic at RT. The iron-silicide layer of sample 2 shows a small average magnetic hf field at 4.2 K of ~ 3.8 T, and ferromagnetism with a small magneticmoment per Fe atom of the order of 0.1 μ_B at 5 K. It appears that such small values of the Fe magnetic moments can only reduce and not destroy the antiferromagnetic interlayer coupling in Fe/FeSi multilayers at low temperature. This is supported by studies of Gareev *et al.*[28] who found that $Fe_{1-x}Si_x$ spacers with a lower Si content of $x \sim 0.36$ [equivalent to a higher Fe content $(1-x)$ of 0.64], which results in larger Fe magnetic moments,[3] are necessary to fully destroy antiferromagnetic interlayer coupling and to obtain ferromagnetic coupling.

We conclude that it is the observed weak ferromagnetism of c-FeSi at low temperature that leads to the reported decrease of the bilinear and biquadratic coupling coefficients in Fe/c-FeSi/Fe trilayers at low temperatures.[11] The present results could explain why in Ref. 11 "part of the paramagnetic entities become ineffective in mediating the biquadratic coupling between the ferromagnetic layers" at low temperatures, namely, because these "loose spins" order ferromagnetically.

IV. CONCLUSIONS

We have successfully synthesized metastable c-FeSi by MBE. Nominal $^{57}FeSi_{0.85}$ films (Fe excess of 15%) were grown by MBE on MgO(100) with a Fe buffer layer (sample 1) or a Cr buffer layer (sample 2). The formation of the c-FeSi phase upon isochronal annealing was observed by CEMS after annealing at 250 °C (sample 1) and 310 °C (sample 2), respectively. X-ray diffraction confirmed the B2 structure of the c-FeSi phase formed in both samples after annealing. For the lattice spacing perpendicular to the surface, a value of 2.77(5) Å at RT for both samples was deduced. At RT, the CEM spectra of the nominal c-$FeSi_{0.85}$ films were fitted with two spectral contributions: (i) a doublet D1 representing the nonmagnetic stoichiometric c-FeSi phase, and (ii) a component with a magnetic hf field distribution, $P(B_{hf})$, characterizing the nonstoichiometric c-FeSi$_x$ phase. This interpretation is supported by EDX results, demonstrating the formation of lateral areas with both, stoichiometric c-FeSi (B2 structure) and nonstoichiometric c-FeSi$_x$ with excess Fe (B2 structure). With decreasing temperature down to 4.2 K, the relative spectral area of the component with the $P(B_{hf})$ distribution increases remarkably at the expense of doublet D1 due to magnetic ordering. The considerable increase of the average hf field observed upon cooling below 28 K can be attributed to magnetic ordering effects of the stoichiometric c-FeSi phase. The conclusions drawn from the Mössbauer results are supported by SQUID magnetometry. Our results prove that both Fe-Si phases are ferromagnetically ordered below 28 K. The Curie temperature was found to be $T_C = 405$ K for the nonstoichiometric c-FeSi$_x$ phase and $T_C = 28$ K for the stoichiometric c-FeSi phase. The observed relatively small saturation hf fields of $\sim 2-4$ T reveal rather weak atomic Fe magnetic moments of the order of $\sim 0.1-0.3$ μ_B. The combination of magnetometry and Mössbauer spectroscopy allows one to determine the ground state magnetic moments per Fe atom to be μ_{Fe}(c-FeSi) $= (0.10 \pm 0.02)$ μ_B and μ_{Fe}(c-FeSi$_x$) $= (0.13 \pm 0.03)$ μ_B. The ferromagnetic ordering of small Fe moments in c-FeSi and c-FeSi$_x$ observed here is very likely the reason for the reduction of the antiferromagnetic interlayer exchange coupling at low T in Fe/c-FeSi/Fe trilayers reported recently.[11]

It is a challenge for theory to confirm the observed small local Fe magnetic moment in c-FeSi in the ground state by spin-resolved electronic band-structure calculations. It is known from theory that c-FeSi exhibits a pronounced peak in the electronic density of states just above the Fermi energy, E_F.[29–31] Structural changes and confinement effects in thin c-FeSi films might modify the electronic properties toward weak ferromagnetism. In fact, the appearance of Fe magnetic moments at Fe-terminated surfaces of c-FeSi has been theoretically predicted recently by Profeta *et al.*[32] Further theoretical work is required to understand the weak ferromagnetism observed in c-FeSi thin films.

ACKNOWLEDGMENTS

We are grateful to U. v. Hörsten (Duisburg) for valuable technical assistance, and H. Nowak and P. Hinkel (Duisburg) for performing EDX measurements. Work was supported by the Deutsche Forschungsgemeinschaft (Grants No. Ke 273/18-1, No. GRK 277, and No. SFB 491).

*Corresponding author. E-mail address: keune@uni-duisburg.de

[1] T. B. Massalski, *Binary Alloy Phase Diagrams* (American Society for Metals, Metals Park, OH, 1986), p. 1772.
[2] H. von Känel, C. Schwarz, S. Goncalves-Conto, E. Müller, L. Miglio, F. Tavazza, and G. Malegori, Phys. Rev. Lett. **74**, 1163 (1995).
[3] D. Berling, G. Gewinner, M. C. Hanf, K. Hricovini, S. Hong, B. Loegel, A. Mehdaoui, C. Pirri, M. H. Tuilier, and P. Wetzel, J. Magn. Magn. Mater. **191**, 331 (1999).
[4] G. J. Strijkers, J. T. Kohlhepp, H. J. M. Swagten, and W. J. M. de Jonge, Phys. Rev. B **60**, 9583 (1999).
[5] Y. Endo, O. Kitakami, and Y. Shimada, Phys. Rev. B **59**, 4279 (1998).
[6] M. Fanciulli, G. Weyer, A. Svane, N. E. Christensen, H. von Känel, E. Müller, N. Onda, L. Miglio, F. Tavazza, and M. Celino, Phys. Rev. B **59**, 3675 (1999).
[7] H. von Känel, K. A. Mäder, E. Müller, N. Onda, and H. Sirringhaus, Phys. Rev. B **45**, 13807 (1992).
[8] S. Degroote, A. Vantomme, J. Dekoster, and G. Langouche, Appl. Surf. Sci. **91**, 72 (1995).
[9] H. Reuther, Surf. Interface Anal. **22**, 547 (1994).
[10] H. Reuther, Hyperfine Interact. **161**, 95 (1995).
[11] B. Croonenborghs, F. M. Almeida, C. Labbé, R. R. Gareev, M. Rots, A. Vantomme, and J. Meersschaut, Phys. Rev. B **71**, 024410 (2005).
[12] J. Dekoster, A. Vantomme, S. Degroote, R. Moons, and G. Langouche, Mater. Res. Soc. Symp. Proc. **382**, 72 (1995).
[13] J. J. de Vries, J. Kohlhepp, F. J. A. den Broeder, R. Coehoorn, R. Jungblut, A. Reinders, and W. J. M. de Jonge, Phys. Rev. Lett. **78**, 3023 (1997).
[14] J. Slonczewski, J. Appl. Phys. **73**, 5957 (1993).
[15] *Mössbauer-Spectroscopy*, edited by U. Gonser, Topics in Applied Physics Vol. 5 (Springer, New York, 1975).
[16] M. Walterfang, W. Keune, and H. Reuther, Phase Transitions **76**, 437 (2003).
[17] R. A. Brand, Nucl. Instrum. Methods Phys. Res. B **28**, 398 (1987). The NORMOS program is available from Wissel GmbH, D-82319 Starnberg, Germany.
[18] J. Hesse and A. Rubartsch, J. Phys. E **7**, 526 (1974).
[19] M. Fanciulli and G. Weyer, Phys. Scr., T **T54**, 16 (1994).
[20] B. Croonenborghs, F. M. Almeida, S. Cottenier, M. Rots, A. Vantomme, and J. Meersschaut, Appl. Phys. Lett. **85**, 200 (2004).
[21] E. P. Elsukov, G. N. Konygin, V. A. Barinov, and E. V. Voronina, J. Phys.: Condens. Matter **4**, 7597 (1992).
[22] G. Marchal, Ph. Mangin, M. Piecuch, and Chr. Janot, J. Phys. Colloq. **37**, 763 (1976).
[23] Ph. Mangin and G. Marchal, J. Appl. Phys. **49**, 1709 (1978).
[24] M. Miyazaki, M. Ichikawa, T. Komatsu, and K. Matusita, J. Appl. Phys. **71**, 2368 (1992).
[25] M. B. Stearns, Phys. Rev. **129**, 1136 (1963).
[26] P. C. M. Gubbens, J. H. F. Apeldorn, A. M. van der Kraan, and K. H. J. Buschow, J. Phys. F: Met. Phys. **F4**, 921 (1974).
[27] G. K. Wertheim, J. H. Wernick, and D. N. E. Buchanan, J. Appl. Phys. **37**, 3333 (1966).
[28] R. R. Gareev, D. E. Bürgler, M. Buchmeier, D. Olligs, R. Schreiber, and P. Grünberg, Phys. Rev. Lett. **87**, 157202 (2001).
[29] Z. Shi, P. M. Levy, and J. L. Fry, Europhys. Lett. **26**, 473 (1994).
[30] E. G. Moroni, W. Wolf, J. Hafner, and R. Podloucky, Phys. Rev. B **59**, 12860 (1999).
[31] J. M. Pruneda, R. Robles, S. Bouarab, J. Ferrer, and A. Vega, Phys. Rev. B **65**, 024440 (2001).
[32] G. Profeta, S. Picozzi, A. Continenza, and R. Podloucky, Phys. Rev. B **70**, 235338 (2004).